Analysing NDVI for the African continent using the geostationary meteosat second generation SEVIRI sensor

Rasmus Fensholt [a,*], Inge Sandholt [b], Simon Stisen [b], Compton Tucker [c]

[a] Institute of Geography, University of Copenhagen, Øster Voldgade 10, DK-1350 Copenhagen, Denmark
[b] Institute of Geography, University of Copenhagen, Denmark
[c] NASA Goddard Space Flight Center, Greenbelt Maryland, United States

Abstract

This study presents first results on Normalized Difference Vegetation Index (NDVI), from the Spinning Enhanced Visible and Infrared Imager (SEVIRI) sensor onboard the geostationary satellite Meteosat Second Generation (MSG) covering the African continent. With a temporal resolution of 15 min MSG offers complementary information for NDVI monitoring compared to vegetation monitoring based on polar orbiting satellites. The improved temporal resolution has potential implications for accurate NDVI assessment of the African continent; e.g. the increased amount of available scenes are expected to help overcome problems related to cloud cover which makes the MSG data particularly well suited for early warning systems. Time series of 2004 MSG NDVI was compared to MODIS (Moderate Resolution Imaging Spectroradiometer) Terra and Aqua NDVI for the Dahra site in the Senegalese Sahel, West Africa. It was found that NDVI was available for 82 days with multiple cloud free acquisitions per day during the growing season as compared to 47 days with information from either MODIS Terra or Aqua for that particular site. Differences in MSG SEVIRI and MODIS BRDF on a seasonal scale were found to influence the time series of NDVI for the test site; MSG NDVI being higher than MODIS in July–August and lower in October–November. Preliminary composite analysis suggests that the period of compositing to produce continent scale cloud free products can be reduced to ~5 days using MSG NDVI as compared to polar orbiting data. With the availability of diurnal reflectance information the significance of differences between the red and near-infrared wavelengths due to anisotropy become evident, causing diurnal variations in observed NDVI. Diurnal MSG NDVI was compared to in situ measured MSG NDVI at the test site in Senegal and the same "bowl-shaped" diurnal curve was found for a medium dense cover of annual grasses. The range in observed NDVI and time of diurnal minimum was different due to different viewing geometry. Daily minimum of in situ measured NDVI was around solar noon whereas minimum MSG NDVI occurs one hour prior to noon due to the test site location 12° west of the satellite sensor. Diurnal variation in observed NDVI was studied for a number of pixels characterized by different sensor view zenith angles and vegetation types. This analysis illustrated the diurnal NDVI dependency of illumination conditions, view angle and vegetation intensity and pinpoints the importance of proper BRDF modeling to produce daily values of MSG NDVI normalized for acquisition time, which will be the subject of a forthcoming paper.
© 2006 Elsevier Inc. All rights reserved.

Keywords: Africa; Geostationary; In situ measurements; NDVI; MSG; Vegetation monitoring

1. Introduction and background

With the launch of the geostationary Meteosat Second Generation, Meteosat-8 satellite with its Spinning Enhanced Visible and Infrared Imager (SEVIRI), unprecedented data for scientific exploration are now available to Earth System Scientists. The MSG program by ESA and EUMETSAT with its planned three identical satellites is expected to remain operational for at least 12 years (Schmetz et al., 2002). The SEVIRI sensor detects radiation in 12 spectral bands among which two are specifically suited for vegetation studies. MSG data have the great advantage over data from the polar orbiting satellites that the frequency of observations is so much higher (15 min interval versus one time a day acquisitions), thus the chances to avoid cloud cover are much improved, which open up for a new vegetation monitoring scheme, in particular for the African continent over which MSG is located. Data from polar

* Corresponding author. Fax: +45 35322501.
  E-mail address: rf@geogr.ku.dk (R. Fensholt).

orbiting satellite sensors have been used extensively for vegetation monitoring during the last decades based on spectral vegetation indices, in particular the Normalized Difference Vegetation Index, NDVI. Consistent global data sets dating back to the early 80's have been generated based on for instance the NOAA AVHRR sensor, like the Pathfinder AVHRR Land data set (PAL) (James & Kalluri, 1994), the Global Inventory Monitoring and Modeling Studies (GIMMS) (Tucker et al., in press), and data from the SPOT VEGETATION sensor (SPOT Vegetation user's guide, 2004). These data sets have been widely used by the scientific geo-biophysical community addressing questions related to global environmental change issues, for instance Nemani et al. (2003). On regional and local scales, remote sensing of vegetation is used for drought early warning and for assessment of plant productivity, or long-term environmental change (Eklundh & Olsson, 2003). Some of the inherent problems encountered with polar orbiting data for vegetation monitoring like cloud contamination or variations due to angular dependence of reflectance (Holben & Fraser, 1984) may be overcome by using data from geostationary satellites; or results can potentially be even further improved by combining data from polar orbiting satellites and geostationary observations (van Leeuwen & Roujean, 2002) giving the possibility of multi view angle data (Roberts, 2001). In recent years data from multi-angle instruments like MISR (Multi-angle Imaging SpectroRadiometer) (Diner et al., 1998) onboard Terra and POLDER (Polarization and Directionality of Earth's Reflectances) on the ADEOS (Advanced Earth Observing System) satellite have opened up possibilities of studying the reflectance of the Earth's surface from varying view angles (Deschamps et al., 1994); a situation complementary to the MSG SEVIRI data source where the target view angle is fixed and the solar zenith and azimuth angles vary. Data from the multi-angle instruments have been used to infer information about vegetation structure and "hot spot" signatures (Gobron et al., 2004; Grant et al., 2004; Lacaze et al., 2002; Pinty et al., 2002).

The results presented here focus on the improved temporal resolution in NDVI from the SEVIRI and the information related to surface anisotropic reflectance that can be extracted from geostationary data. The results point towards the subject of daily NDVI compositing techniques, which needs to be resolved, in particular related to the anisotropy of the surface and to diurnal variation. With a 15 min temporal resolution in data it is now possible to obtain diurnal information of NDVI from the red and near-infrared reflectances with a spatial coverage for the entire African continent. In this study, the use of MSG SEVIRI data for assessment of vegetation cover is explored for the African continent based on data from 2004 and selected days in 2005. The objectives of the paper are to illustrate some of the potential of using SEVIRI data for large scale NDVI mapping as a complementary data source to polar orbiting satellites, and, in particular, to pinpoint the basic performance of SEVIRI NDVI data stressing the special features of geostationary data. The processing chain for SEVIRI data implemented at the Institute of Geography, University of Copenhagen is presented, including calibration, geometric rectification and atmospheric correction of red, near-infrared and SWIR channels. The performance of SEVIRI data in comparison to MODIS with regards to cloud free daily NDVI data is illustrated. The relation to in situ measurements of surface reflectance in similar bandwidths from an automatic station at the Dahra test site (Fensholt & Sandholt, 2005) in the Northern, semi-arid part of Senegal in West Africa is shown, and the effect of illumination and viewing geometry are addressed. The paper is concluded by outlining future areas of work based on the findings of the study.

1.1. Vegetation index

Vegetation is traditionally monitored using information from the red (high absorption) and near-infrared wavelengths (high reflectance) combined into the Normalized Difference Vegetation Index (NDVI) (Myneni et al., 1995; Tucker, 1979). NDVI is defined as:

$$NDVI = \frac{NIR - RED}{NIR + RED}$$

Where NIR is reflectance in the near-infrared wavelengths and RED is reflectance in the red wavelengths.

The applicable satellite data for estimation of NDVI have so far been based on polar orbiting satellites carrying sensors detecting radiation in red and near-infrared wavelengths. Much effort has been put into development of improved measures of vegetation — in particular improvements in spectral resolution of new sensors have been in focus with the American MODIS sensor (Huete et al., 1999) and the European MERIS sensor (Gobron et al., 2004). This has made estimation of new vegetation indices, like EVI from the MODIS sensor (Huete et al., 2002) and MGVI from the MERIS sensor, possible. Despite daily image acquisitions from the polar orbiting satellites, a much lower frequency of successful image acquisitions can normally be obtained due to the presence of cloud cover. Temporal composites of NDVI values on a scale from 10 to 16 days are applied to minimize the effects of clouds and atmospheric influence from aerosols and water vapour (Holben, 1986); however, during the Sahelian Africa growing season it is often the case that composites period lengths of 10 to 16 days may not be able to capture the dynamics of the vegetation because of persistent cloud cover (Fensholt et al., submitted for publication). The high temporal frequency of SEVIRI increases the chance of obtaining cloud free image data and daily NDVI data may in many cases now be available.

1.2. The bidirectional reflectance distribution function (BRDF)

The anisotropic behaviour of reflectance from most natural surfaces is a complication in using both polar orbiting and geostationary satellite data for vegetation studies, because anisotropy influences observations unevenly for varying sun-view geometry. Several recent studies of sensitivity of spectral reflectance to satellite viewing geometry and solar illumination angles have documented a very large dependence and variation

in Bidirectional Reflectance Distribution Function (BRDF) (Gao et al., 2002). In particular data from the POLDER instrument have been useful in the assessment of BRDF (e.g. Hautecoeur & Leroy, 1998; Leroy et al., 1997). Work in order to derive land surface albedo based on SEVIRI data has been reported in the literature (Geiger et al., 2004; Pokrovsky et al., 2003), work that necessarily involves modeling of the BRDF. Several physically and empirically based models have been developed to deal with the significance of BRDF on surface reflectances (Li & Strahler, 1986; Myneni et al., 1992). Analysis of the bidirectionality of NDVI however lags far behind (Gao et al., 2002). The BRDF is wavelength dependent, and vary with land cover type, consequently, the normalizing effects on NDVI will not fully account for the influence of scene geometry.

Differences in bidirectional reflectance for a vegetated pixel are primarily caused by shadowing effects due to the geometry of the canopy (Hapke et al., 1996). Reflectance in the red wavelength is found to be strongly anisotropic (non-Lambertian reflectance characteristics) compared to the near-infrared wavelengths (Huete et al., 1992) when monitoring partial canopy cover as a function of view and solar zenith angles. The strongest reflection in red wavelength is found in the backscatter direction because the canopy and soil are illuminated, whereas reflection in the forward scatter direction is weaker since a larger part of the vegetation and soil are shadowed. "Hot spot" conditions occur when the phase angle between sun and sensor tends to zero (the sun and sensor being in the principal plane with identical zenith angles), thereby strongly illuminating the vegetation and soil surface. Reflectance in the near-infrared wavelengths is by contrast more isotropic for a densely vegetated surface, being only slightly stronger in the backscatter direction. The preservation of near-infrared reflection in the forward scatter direction compared to the properties in red wavelength domain is caused by a larger part of near-infrared radiation being transmitted through canopies and thereby reflected by soil and leaves (Cihlar et al., 1994). Calculating NDVI from red and near-infrared reflectance for vegetated surfaces, the combination of low reflectance in red forward scatter direction and relatively high reflectance in near-infrared forward scatter direction results in higher observed NDVI values in the forward scatter direction compared to the backward scatter direction. Bidirectional NDVI for homogeneous vegetated surfaces generally shows a bowl-shaped feature, with increasing NDVI values for increasing sun and view zenith angles depending on the vegetation structure and the atmospheric composition (Gao et al., 2002; Widlowski et al., 2004) when modeled from radiative transfer models (Goward & Hummrich, 1992; Huete et al., 1992; Myneni et al., 1992) or measured by ground bidirectional reflectance instruments (Deering et al., 1992; Sandmeier and Itten, 1998).

These considerations apply for varying view zenith angles (VZA) of the SEVIRI sensor when comparing pixels of different VZA's from the same scene. However, when monitoring diurnal surface reflectance from a given pixel the variations in reflectances are caused by variations in solar zenith and azimuth angles; a situation complimentary to Polar Orbiting Environmental Satellites (POES), because POES operate in sun synchronous orbits and variations in sun zenith angle in the course of the year go along with the variations in the vegetation cycle. Geostationary data have been used to assess information on surface anisotropy (d'Entremont et al., 1999) but this is the first paper introducing NDVI from a geostationary satellite including results analyzing diurnal variation in observed NDVI from a fixed view position with varying solar zenith angles.

2. The SEVIRI sensor and data

The MSG satellite was launched on 29th of August 2002 and, after the commissioning phase, the satellite was put into its nominal operational position at 3.4° West longitude at an altitude of 36.000 km. Routine operations with MSG-1 started 28th of January 2004 and since then, data have been available to the scientific community (Hanson & Mueller, 2004). The SEVIRI sensor is equipped with 12 spectral channels, ranging from visible wavelengths to far infrared wavelengths (Table 1).

MSG is a spin-stabilized satellite, and imaging is performed by combining satellite spin and rotation of the scan mirror. A nominal repeat cycle is ~12 min (Schmetz et al., 2002) and radiometric discritization of the 12 channels is 10 bits. Spatial sampling at the sub-satellite point is 3 km, and the spatial resolution (instantaneous field of view (IFOV)) is 4.8 km, except for the HRV channel (Schmetz et al., 2002). The spatial resolution varies with viewing geometry, reaching 5–6 km in the Southern and Eastern parts of the African continent (EUMETSAT, 2005). Coregistration of the multi-spectral images is better than 0.6 km for the visible and near-infrared channels and coregistration of multi temporal images is done with an accuracy of better than 1.2 km. Tests during the commissioning and initial routine phases have shown that the MSG SEVIRI sensor delivers data of excellent quality (Teianu et al., 2004).

Several application areas have been foreseen, for terrestrial applications the bands in the Visible (0.6), Near-infrared (0.8) and Short Wave Infrared (1.6) are interesting for assessment of vegetation parameters. In the near future, the possibility of further improvements to the accuracies is expected, due to the potential of getting information about atmospheric constituents giving input to atmospheric correction algorithms.

Table 1
Characteristics of the SEVIRI sensor onboard MSG

SEVIRI band nr	Spectral range (μm)	Centre (μm)	Spatial sampling at sub-satellite point (km)
1 (VIS 0.6)	0.56–0.71	0.635	3
2 (VIS 0.8)	0.74–0.88	0.81	3
3 (IR 1.6)	1.50–1.78	1.64	3
4 (IR 3.9)	3.48–4.36	3.92	3
5 (WV 6.2)	5.35–7.15	6.25	3
6 (WV 7.3)	6.85–7.85	7.35	3
7 (IR 8.7)	8.30–9.10	8.70	3
8 (IR 9.7)	9.38–9.94	9.66	3
9 (IR 10.8)	9.80–11.80	10.80	3
10 (IR 12.0)	11.00–13.00	12.00	3
11 (IR 13.4)	12.40–14.40	13.4	3
12 (High resolution VIS)	0.50–0.90	0.75	1

3. MSG data preprocessing

At the Institute of Geography, University of Copenhagen, a prototype of an operational real time MSG SEVIRI processor has been build and tested in WinCHIPS (Hansen, 2001), and an optimized version of the processor is currently being re-written in IDL. Output from the processor is atmospheric corrected (see below) reflectance in bands 1 (0.56–0.71 μm) and 2 (0.74–0.88 μm), which are used for calculation of NDVI. The prototype also handles the short wave infrared channel 3 (1.50–1.78 μm) and infrared channels of MSG SEVIRI for assessment of surface temperature; this will be described in a forthcoming paper. The processor takes Level 1.5 MSG SEVIRI data as delivered by EUMETSAT via the EUMETCast service. The level 1.5 data are retransmitted in the HRIT format via a commercial satellite, Hotbird 6, to the EUMETSAT facility in Darmstadt Germany. The HRIT format SEVIRI data are composed of 3712 by 3712 pixels for all channels except HRV with a sampling distance of 3 by 3 km at the sub-satellite point. Images are represented as 10 bit data (EUMETSAT, 2004).

At the reception station at the Institute of Geography, University of Copenhagen, the MSG SEVIRI data are received near real time through the mandatory TELLICAST client software (EUMETSAT, 2004). Further file handling is carried out using the MSG Data Manager Pro version (Taylor, 2005), which automatically handles all incoming data producing uncompressed 10 bit MSG SEVIRI images. The raw data are computed into reflectance (channels 1–3) and brightness temperature (channels 4–11) by using algorithms similar to the implementation in "SEVIRI NATIVE format pre-processing toolbox" (Govaerts et al., 2005). For reasons of simplicity and processing speed the exact acquisition time of each line is interpolated over the 3712 lines assuming a total scan time of 12 min and 40 s. Although the scanning process is more complicated than indicated here, the simplification will not result in any significant error in the calculations of sun geometry associated with the computation of reflectance for the visible channels. All band and sensor specific constants are taken from the "SEVIRI NATIVE format pre-processing toolbox" and image calibration slope and offset are read from the image header information.

The reflectance and brightness temperature images are subsequently georectified to a relevant geographical map projection with a pixel spacing of three kilometers and saved as 16 bit integer images.

3.1. MSG atmospheric correction

The atmospheric correction of the red, near-infrared and SWIR bands from Top Of Atmosphere (TOA) reflectances into surface values is done using the SMAC algorithm (a Simplified Method for the Atmospheric Correction of satellite measurements in the solar spectrum) (Rahman & Dedieu, 1994), an approach used by the Land SAF as well (Geiger et al., 2004). SMAC is a simple and fast technique based on the 5 S code applicable to a range of satellite sensors and it accounts for atmospheric absorption and scattering due to gaseous constitutions and aerosol content of the atmosphere. We have used the coefficients developed by Beatrice Berthelot (Berthelot, 2003), for the three channels. The accuracy of the SMAC code decreases for solar zenith angles greater than 60°, for viewing angles greater than 50°, and for optical depths greater than 0.8 at 550 nm (Rahman & Dedieu, 1994). Thus, the algorithm is applicable for SEVIRI data for the major part of the African continent; view angles larger than 50° are found in the fringes of the continent only (see Fig. 7).

Daily values of atmospheric composition (water vapour, aerosols, and ozone) are derived from the Level-3 MODIS Terra and Aqua Atmosphere Daily Global Products, which are sorted into $1 \times 1°$ cells on an equal-angle grid. The atmospheric data layers used in the current atmospheric correction of the channels 1, 2 and 3 are listed in Table 2. Ideally water vapour, aerosols, and ozone should be derived directly from SEVIRI data enabling an accurate temporal correspondence between the scene to be corrected and atmospheric input data for correction. At present time the MODIS data are however the best solution even though diurnal variations in water vapour and aerosols occur; potentially introducing inaccuracies in the diurnal range of observed NDVI.

The estimate of errors in retrieving the total atmospheric water vapour and total ozone are both 10% (Menzel & Gumley, 1998) and the aerosol optical thickness (τ_a) can be sensed with an estimated error of $\tau_a = 0.05$ to 0.1 for small optical thickness, increasing to 20–30% for high optical thickness (Kaufman & Tanre, 1998). Daily composites of the entire African continent are performed from the MODIS Terra morning and Aqua afternoon over pass by simple averaging. A standard distribution filter is applied to fill out data gaps generated by the orbital coverage of Terra or Aqua data and finally data are resampled by bilinear interpolation to match the MSG SEVIRI pixel size.

A sensitivity analysis on the SMAC algorithm was performed. Varying ozone content within the typical range occurring during the year (0.22–0.28 cm atm.) has minimal influence on observed NDVI. The atmospheric water vapour content has larger impact on observed NDVI; varying atmospheric water vapour from 1 to 6 g/cm which are the extremes found for the African continent; produces variations in NDVI of ±0.01. It was found that observed NDVI is most sensitive to variations in aerosol optical thickness. Varying the aerosol load between 0.1 and 0.8 (unitless) for low solar zenith angles (0–20°) produces variations in observed NDVI of ±0.05 for dense vegetation. When the solar zenith angle is increased to above 30° the observed NDVI variation for a densely vegetated pixel increases to approximately ±0.1.

Table 2
MODIS atmospheric data layers used for atmospheric correction of MSG data

Variable	Product	Derived from
Atmospheric water vapor	MOD/MYD08	MOD/MYD 07 L2 SDS
Corrected optical depth land	MOD/MYD08	MOD/MYD 04 L2 SDS
Total ozone	MOD/MYD08	MOD/MYD 07 L2 SDS

3.2. Assessment of NDVI

The Normalized Difference Vegetation Index is calculated from cloud masked surface reflectance in the red and near-infrared channels for each image acquisition. We use the MSG cloud mask distributed with the HRIT data. Acknowledging the solar zenith angle influence on observed NDVI only data from 10 am to 2 pm local solar time are included in these analyses. The diurnal variation of observed NDVI and the selection of a 4-h time interval are subject for further discussion in the subsequent sections of this paper. Descriptive statistics are estimated, and a preliminary estimate of daily NDVI is made from a simple averaging of the images from 10 am to 2 pm local solar time.

The full processing chain from Level 1.5 product received via EUMETCast to the final NDVI images is shown in Fig. 1 and Table 3 summarizes the different data sources used for NDVI estimates in the analysis.

4. Results and discussion

4.1. Improvements in image frequency and comparison to in situ measurements

Time series of MSG SEVIRI NDVI (10 am–2 pm local solar time) are plotted together with MODIS Terra and Aqua NDVI for the Dahra test site in the Senegalese Sahel (lat 15.40; long −15.43) in the growing season 2004, Fig. 2.

Only cloud free scenes are included as specified by the MODIS quality flags and the MSG cloud mask. Pixel size of MSG SEVIRI NDVI data is 3000 m and the MODIS MOD/MYD09GQK daily 250 m red and near-infrared reflectances have been aggregated to match the MSG SEVIRI spatial pixel resolution before calculation of NDVI.

From the combined use of the Terra (overpass time 10:30 am) and Aqua (overpass time 1:30 pm) data, 47 days of cloud free scenes (either Terra or Aqua) were available at the test site during the 2004-growing season. For comparison 82 days with at least 1 cloud free scene between 10 am and 2 pm were

Table 3
Data sources used for NDVI estimates

	2004	2005
MSG-SEVIRI (3 km)	Red and near-infrared; growing season	20–30 March
MODIS (250 m and 1°)	MOD/MYD08; MOD/MYD09GQK	20–30 March
In situ (point)	Red and near-infrared (growing season NDVI)	

available from MSG SEVIRI. When comparing MSG SEVIRI average NDVI to resampled MODIS Terra/Aqua NDVI a fairly good agreement in the dynamic range was found with a tendency to slightly higher MSG NVDI values in the beginning of the growing season (July–August) and slightly lower towards the end (October–November). This pattern is found for seasonal analyses all across Sahel (not shown) and can be explained by seasonal variations in the solar azimuth angle. In July–August the path of the sun is north of Senegal, creating a forward scatter situation (the location of the sensor being fixed at equator) resulting in higher MSG NDVI values. In October–November the sun passes south of equator thereby creating a backward scatter situation generally lowering the MSG NDVI values. Varying solar azimuth angles evidently also influence MODIS data but due to the nature of polar orbiting data employing a cross-track scanning radiometer the influence appears less distinct compared to the geostationary MSG data.

Fig. 3 summarizes the number of cloud free MSG SEVIRI NDVI scenes from 10 am to 2 pm in the 2004 growing season, yielding a total number of 910. The figure also shows mean values of MSG NDVI with value-axis bars indicating minimum and maximum observed NDVI for the specific days. The range of diurnal MSG SEVIRI NDVI data is a function of the vegetation intensity with larger amplitudes during peak of the growing season, when surface anisotropy is expected to be highest. For two cloud free days in September (characterized by 17 observations) only separated by 4 days (Sept 2 and 6) the MSG NDVI dynamic range is markedly different. There is no evident explanation for this,
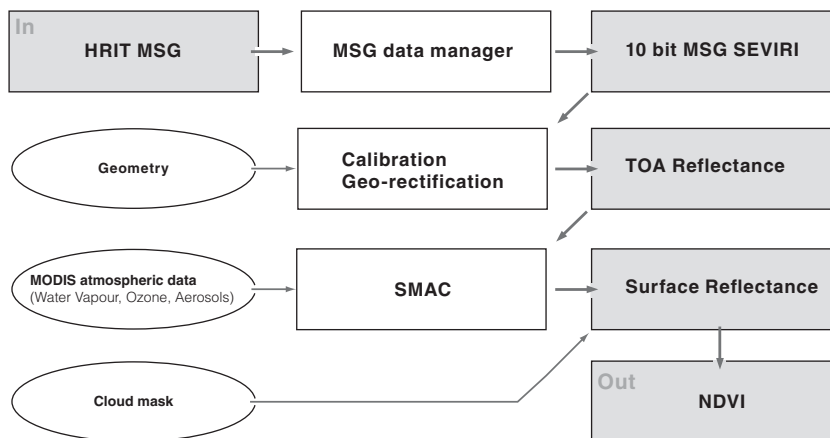
Fig. 1. The MSG (Meteosat Second Generation) SEVIRI (Spinning Enhanced Visible and Infrared Imager) processor as implemented at the Institute of Geography, University of Copenhagen.
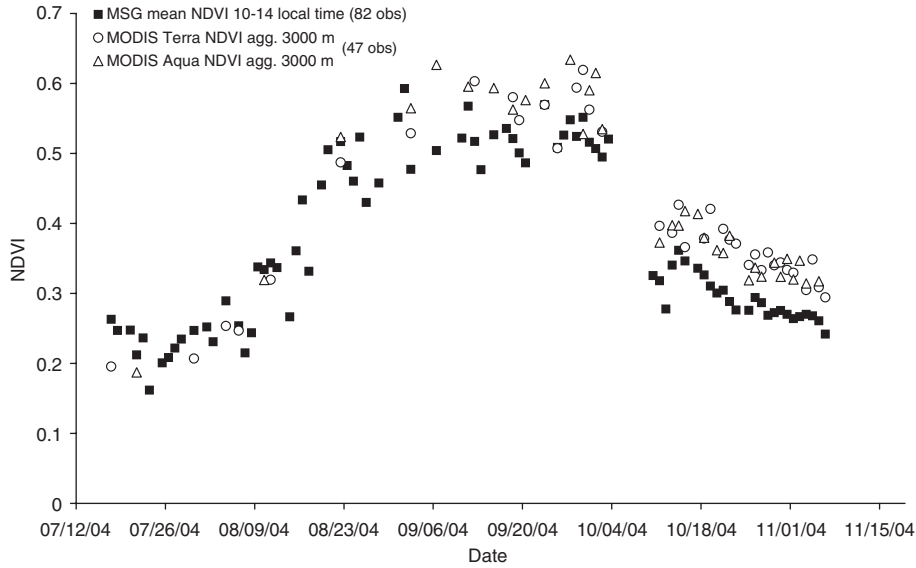
Fig. 2. Mean daily MSG NDVI (Normalized Difference Vegetation Index) for cloud free scenes in a 4 h time window (10 am to 2 pm local time) for the pixel covering the field station in Dahra, Senegal during the 2004 growing season. The number of available daily mean MSG NDVI values (82 days) is compared to the number of days with cloud free MODIS (Moderate Resolution Imaging Spectroradiometer) Terra or Aqua NDVI values (47 days).

but it could be a consequence of using MODIS one time of day atmospheric input in the SMAC algorithm, which is currently the best solution available.

Only 3 days have less than three daily cloud free acquisitions indicating that information from almost all of the 82 days are highly reliable, in the sense that information
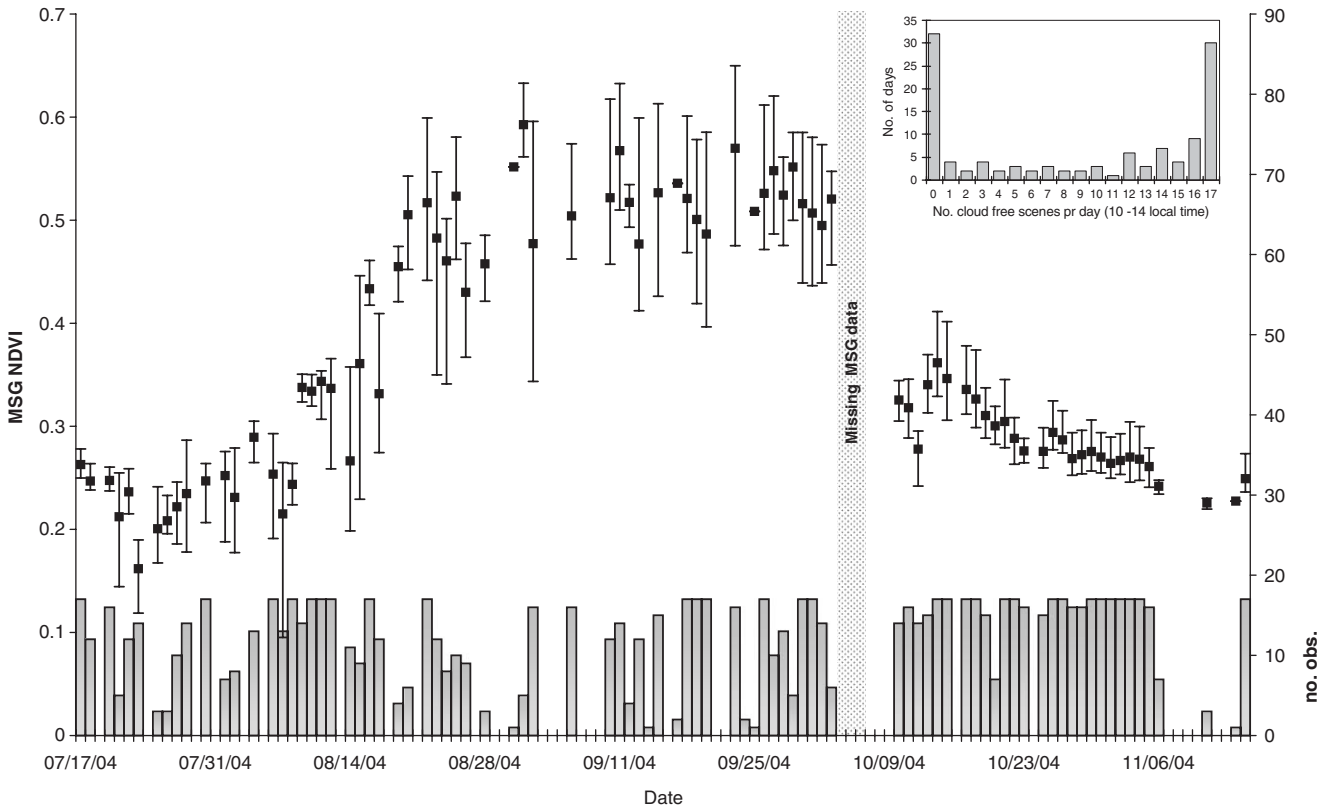
Fig. 3. Mean daily MSG NDVI for cloud free scenes in a 4 h time window (10 am to 2 pm local time) for the pixel covering the field station in Dahra, Senegal during the 2004 growing season (value-axis bars indicate minimum and maximum NDVI values). Bottom columns indicate the number of cloud free daily observations used for the mean NDVI estimate. Upper right corner figure illustrates the histogram of cloud free scenes for the 2004 growing season for the pixel covering the station in Dahra, Senegal.

not influenced by clouds is likely to be available. There are some minor jumps in the MSG NDVI seasonal curve which can be attributed to the simple averaging. If e.g. 5 available observations are all located in the beginning/end of the 4 h period, evidently the simple average value will introduce a bias. A more detailed evaluation of MSG SEVIRI NDVI against MODIS NDVI will be the subject of a forthcoming paper. Using a larger temporal window than between 10 am and 2 pm gives an even higher number of days with NDVI information from the test site. However, the inclusion of NDVI values recorded with high solar zenith angles also introduces higher amplitudes in the diurnal observed NDVI variation with rapidly increasing NDVI in the morning and afternoon due to increasing solar zenith angles. This introduces more noise than information if a thorough normalization is not performed. The more frequent MSG SEVIRI NDVI data means that problems related to cloud cover are reduced, because the probability of seeing the ground surface through any fleeting gaps in cloud cover during daytime is increased. For illustration of the increased spatial coverage where reliable NDVI can be obtained, data from the 29 March 2005 covering the entire African continent are used to calculate the number of cloud free observations during one day. This is shown in Fig. 4(a) together with NDVI for pixels with at least one daily observation (Fig. 4 (b)). To avoid high solar zenith angles in the east–west direction, only a 4 h temporal window of NDVI data centred on local solar noon is allowed (from 10 am to 2 pm). This results in a maximum of 17 scenes for any given location.

4.2. Implications for compositing periods

The temporal resolution of the MSG SEVIRI NDVI and the increased availability of cloud free acquisitions open up the possibility of substantially reducing the composite period length needed to produce cloud free coverage of the African continent as compared to the NDVI studies based on polar orbiting satellites. A preliminary composite analysis is presented here using a 4 h window of data. A simple 10 am to 2 pm daily NDVI average of cloud free scenes is performed on data covering March 20 to March 30 2005. When compositing over more than one day, the maximum of the daily NDVI mean values is selected as originally proposed by Holben (1986). Future work will focus on how to normalize the MSG SEVIRI data to form a more advanced daily NDVI composite value for a given pixel, taking the diurnal variations discussed in the subsequent section into account.

MODIS Terra and Aqua 1 to 10-day composite cloud masks (and MODIS Terra and Aqua combined) for the African continent covering the same time interval are plotted for comparison (Fig. 5a). MODIS Aqua has the lowest percentage of cloud free pixels due to the afternoon equator passing time. The increase in cloud free pixels available with MSG compared to MODIS Terra and Aqua is evident. The number of cloud free pixels from the combined use of Terra and Aqua is only marginally lower than for MSG when

performing the analysis on a 10-day composite period because the benefit of including more days in the composite period is asymptotically decreasing. Statistics for Congo (Fig. 5b) in the central equatorial Africa characterized by permanent high cloud cover elucidates the difference between the number of cloud free MSG and MODIS pixels for this 10-day composite period. For the larger part of the continent characterized by less cloud cover than the central equatorial Africa, the high frequency of MSG data can reduce the number of days needed in a composite period. Reducing the MSG composite period to 5 days instead of 10 days (Fig. 5c) produces two African composite products with only a marginally lower percentage of cloud free pixels than the full 10-day period and the difference in the performance of the MSG and MODIS data stands out more clearly compared to the full 10-day composite period. Analysis of this 10-day period appears very promising for substantially reducing the composite period using MSG NDVI. With adequate diurnal normalization techniques of the MSG data the 4-h temporal window used in this analysis (yielding a maximum of 17 scenes to select from) can be expanded to include considerably more data thereby further increasing the advantages of the 15 min temporal resolution of MSG data. A map of MSG 10-day maximum composite NDVI based on daily average NDVI for the African continent during March 20–30 2005 is given in Fig. 5d. It should be noticed that March 20–30 falls within the northern hemisphere dry season (the majority of land pixels are located on the northern hemisphere part of the African continent); it will be interesting to redo the analysis for data covering the northern hemisphere rainy season in September 2005.

4.3. Effect of illumination and viewing geometry

The position of the geostationary MSG SEVIRI is fixed, hence pixel reflectance is only influenced by changes in the sun position (MSG sensor 10°, 20°, 30°, 40° and 50° view zenith angles are indicated on all maps), compared to polar orbiting satellites with both variations in solar and sensor geometry. Three days of in situ measured (15 min interval) MSG NDVI and the corresponding SEVIRI pixel NDVI are plotted for the Dahra test site in Senegal in Fig. 6.

Bowl-shaped NDVI curves are found for both in situ and satellite data. The amplitude and timing of the curves are however different due to differences in viewing geometry. The ground sensors measuring nadir reflectances exhibit the lowest NDVI values around local solar noon, when sun zenith angle is at its minimum. The pixel, as viewed by the MSG satellite, located 12° west of the sensor is however characterized by a different sun-sensor viewing geometry compared to in situ measurements. The sensor view angle of the pixel is 23° and the sun is behind the sensor approximately in the principal plane approaching a "hot spot" situation at about one hour prior to local solar noon at the test site leading to a one hour displacement in the diurnal minimum in NDVI observations. This clearly illustrates the influence of the sun-sensor geometry on the observed daily
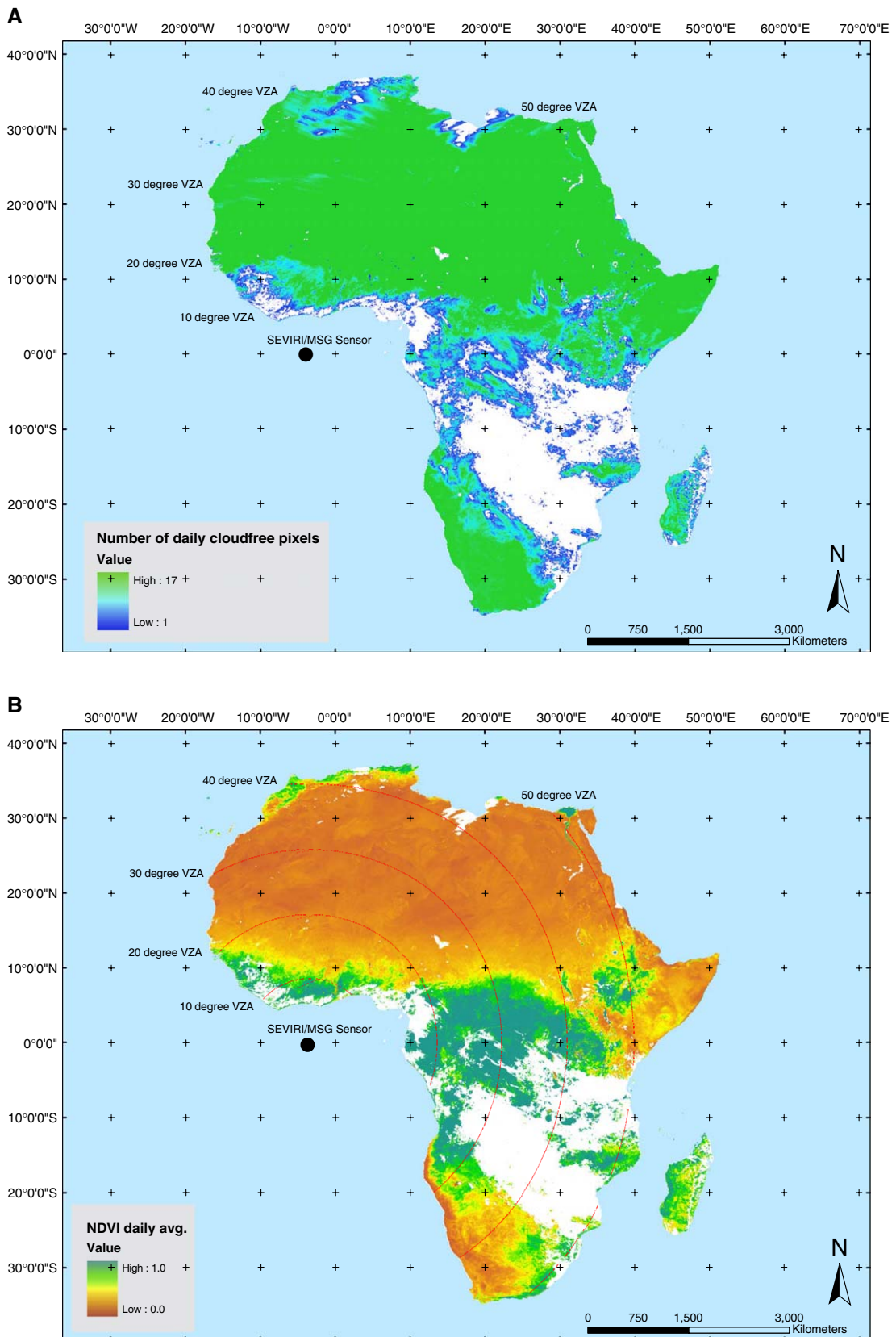
Fig. 4. Map of number of daily cloud free MSG pixels using a 4 h time window (10 am to 2 pm local time; a total of 17 scenes) for the African continent 29/3 2005. White colour represents cloudy conditions in the entire time interval (A). Map of MSG average NDVI for the African continent 29/3 2005 (SEVIRI MSG 10, 20, 30, 40 and 50 view zenith angles indicated with red lines) (B). MSG Data c2005 EUMETSAT.
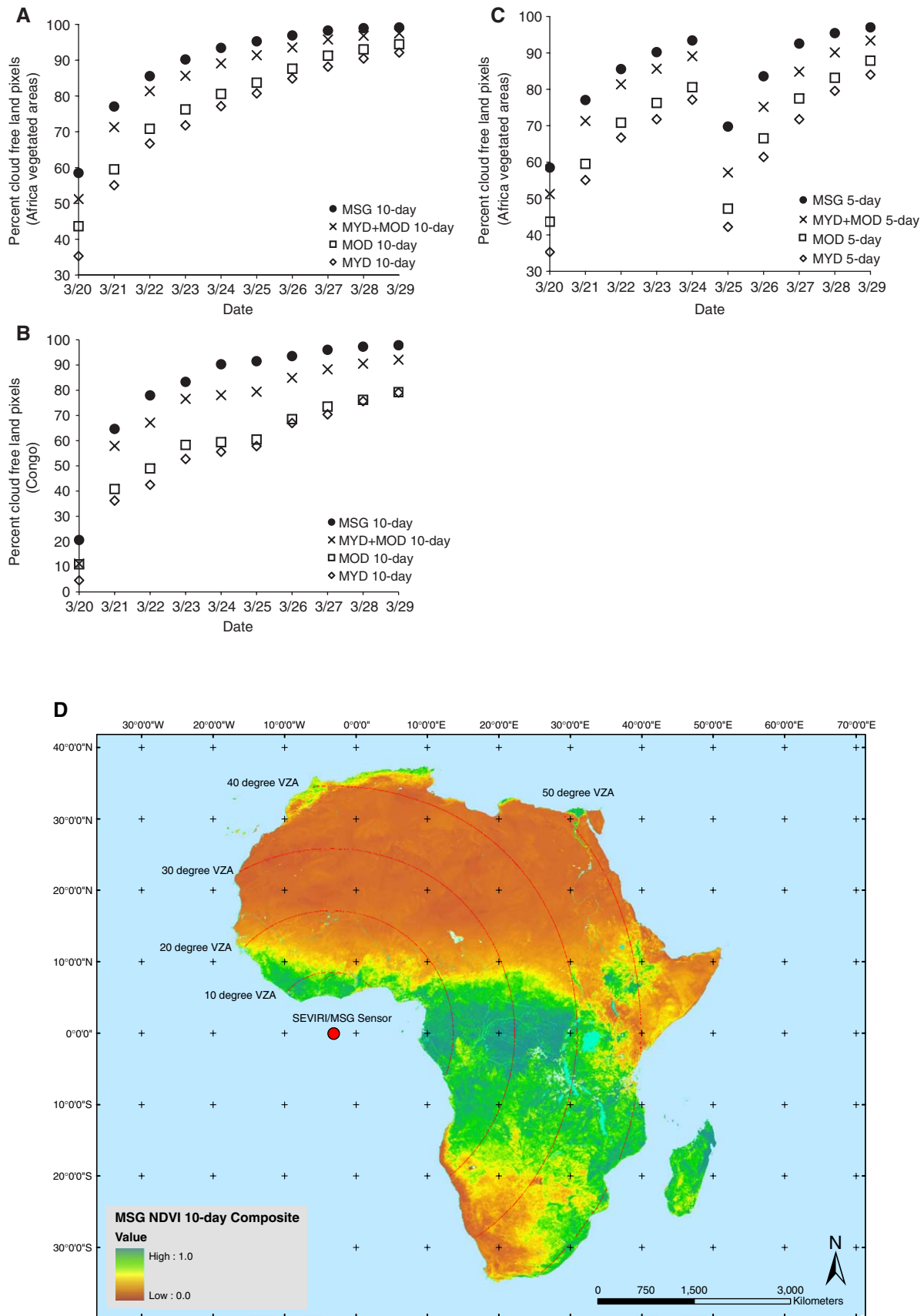
Fig. 5. Percent cloud free land pixels for the African continent for varying composite periods ranging from 1 to 10 days during March 20–30 2005 (A) and for the democratic republic of Congo (B). Percent cloud free land pixels for the African continent for varying composite periods ranging from 1 to 5 days during March 20–30 2005 (C). Map of MSG 10-day maximum composite NDVI based on daily average NDVI for the African continent during March 20–30 2005 (D). MSG Data ©2004 and 2005 EUMETSAT.
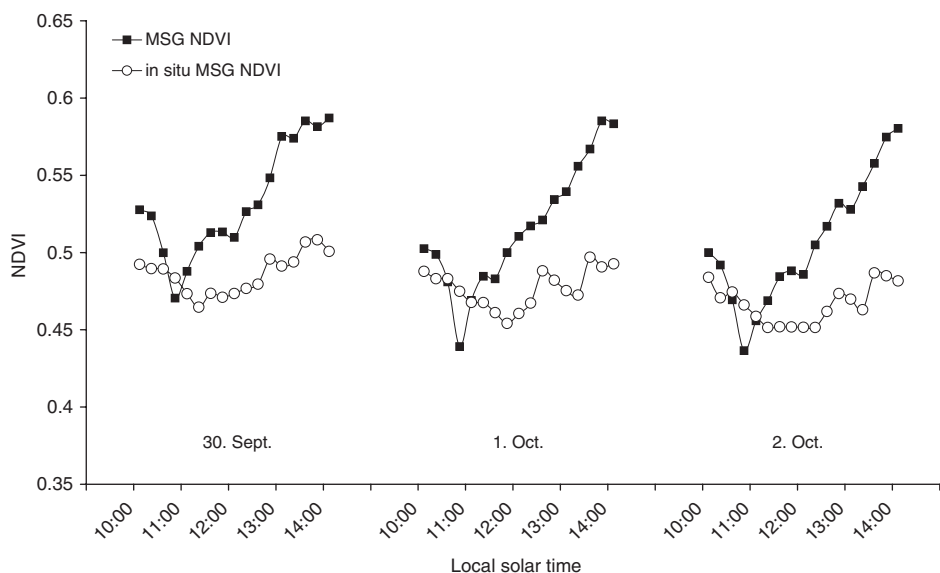
Fig. 6. Diurnal MSG NDVI curves in the 10 am to 2 pm time window for the pixel covering the Dahra field station (MSG view zenith angle of 23°), compared to in situ measurements of MSG NDVI for the same hour but with view zenith angle of 0°.

NDVI variation. The amplitude of the diurnal observed NDVI from the MSG SEVIRI is larger than found for the in situ measured values. This difference might be due to scale or it could be due to the different observation conditions. The last hypothesis will be tested for the Dahra test site in the 2005-growing season where the nadir ground SEVIRI sensor will be supplemented by a SEVIRI sensor mounted with a "tilted" view angle identical to how the pixel is recorded by the MSG SEVIRI sensor.

The influence of the sun-sensor geometry on the NDVI values is further analyzed by studying the diurnal observed NDVI variation for a wide range of sun-sensor viewing geometry and vegetation intensities covering different biomes over the African continent. Also in this analysis a 4 h window of data centred around local solar noon is used to avoid too high solar zenith angles in the east–west direction produces a maximum of approximately 30 degrees solar zenith angles. The IGBP (International Geosphere–Biosphere Program) biome classes (Loveland & Belward, 1997) in combination with iso-lines of sensor view zenith angles of 10–50° and NDVI intensity/cloud cover information (Fig. 7a and b) are used as criterion for selection of sites to analyze.

The cloud free areas in this analysis (Fig. 7b) have been selected such that they are not influenced by clouds at any time between 10 am and 2 pm. Data from the 29/3 2005 was selected for analysis based on a northern hemisphere low cloud cover (representing the majority of land surface pixels). The selected date is close to equinox, meaning that the sun and the sensor are located in same principal plane theoretically causing the BRDF effects to be most pronounced in the areas close to equator. Diurnal MSG SEVIRI NDVI observations corresponding to the geographical locations given by the numbers in Fig. 7b are illustrated in Fig. 8 (MSG SEVIRI sensor view zenith angles (VZA) of 10–20°), and Fig. 10 (VZA's from 30 to 50). The NDVI values are indicated as relative deviations in percent from

the 10 am to 2 pm simple average to ease the comparison of NDVI trajectories covering different vegetation intensities.

4.3.1. Viewing angles from 10° to 20°

Pixels selected from the MSG SEVIRI sensor VZA's from 10 to 20 can potentially be located both west and east of the sensor and thus represent a broad range of different diurnal sun-sensor illumination conditions. Pixels located west of the sensor (pixels 1–2 and 5–8) are characterized by before noon backward scatter illumination conditions, whereas the opposite is the case for pixels located east of the sensor (pixels 3–4 and 10–13). Due to a persistent cloud cover in the southernmost West Africa it is rare to have cloud free conditions during the 4 h from 10 am to 2 pm. This was however the case at the 29/3 2005 for a part of the 10° VZA (Fig. 8), but only for pixels classified as savannas by the IGBP classification (Fig. 7a). Pixels 1 and 2 are characterized by moderately dense vegetation (avg. NDVI of 0.53 and 0.56) and both plots clearly illustrate the bowl-shaped diurnal variation in observed NDVI. The diurnal NDVI minimum is found just before the local solar noon, which is as expected from the geographic location of the two pixels app. 1° west of the sensor. The same bowl-shaped curve is found for pixels 3 and 4 characterized by comparable vegetation intensities and biome type; all plots characterized by a diurnal variation of app. 0.05 NDVI units. However, the observed diurnal NDVI minimum has now shifted to shortly after noon corresponding to a geographic location 2° east of the sensor.

Pixels selected along the MSG SEVIRI 20° VZA span different biome classes and local solar noon can differ more from GMT solar noon generating a diurnal displacement of the backscatter conditions (Fig. 8). Pixels 5–8 represent the biome classes; evergreen forest, woody savannas, savannas and grasslands characterized by decreasing average NDVI values. The bowl-shaped diurnal variation is evident and the dynamic
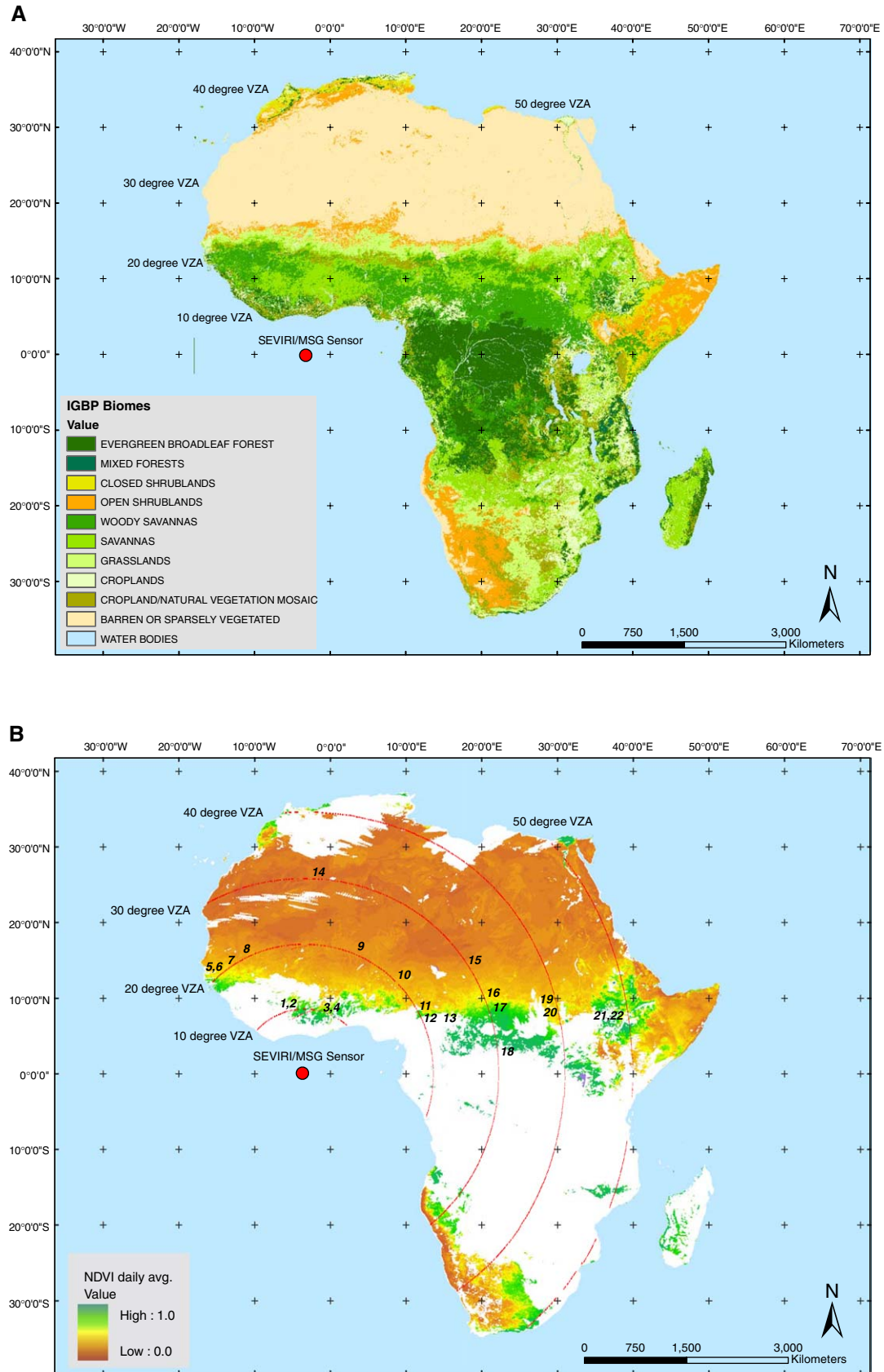
Fig. 7. IGBP (International Geosphere–Biosphere Program) biome classification for the African continent (A). Daily MSG NDVI average for pixels labelled as cloud free in the interval from 10 am to 2 pm local solar noon (29/3 2005). The numbers indicated correspond to pixels where analysis of diurnal NDVI is performed (SEVIRI MSG 10, 20, 30, 40 and 50 view zenith angles indicated with red lines) (B).
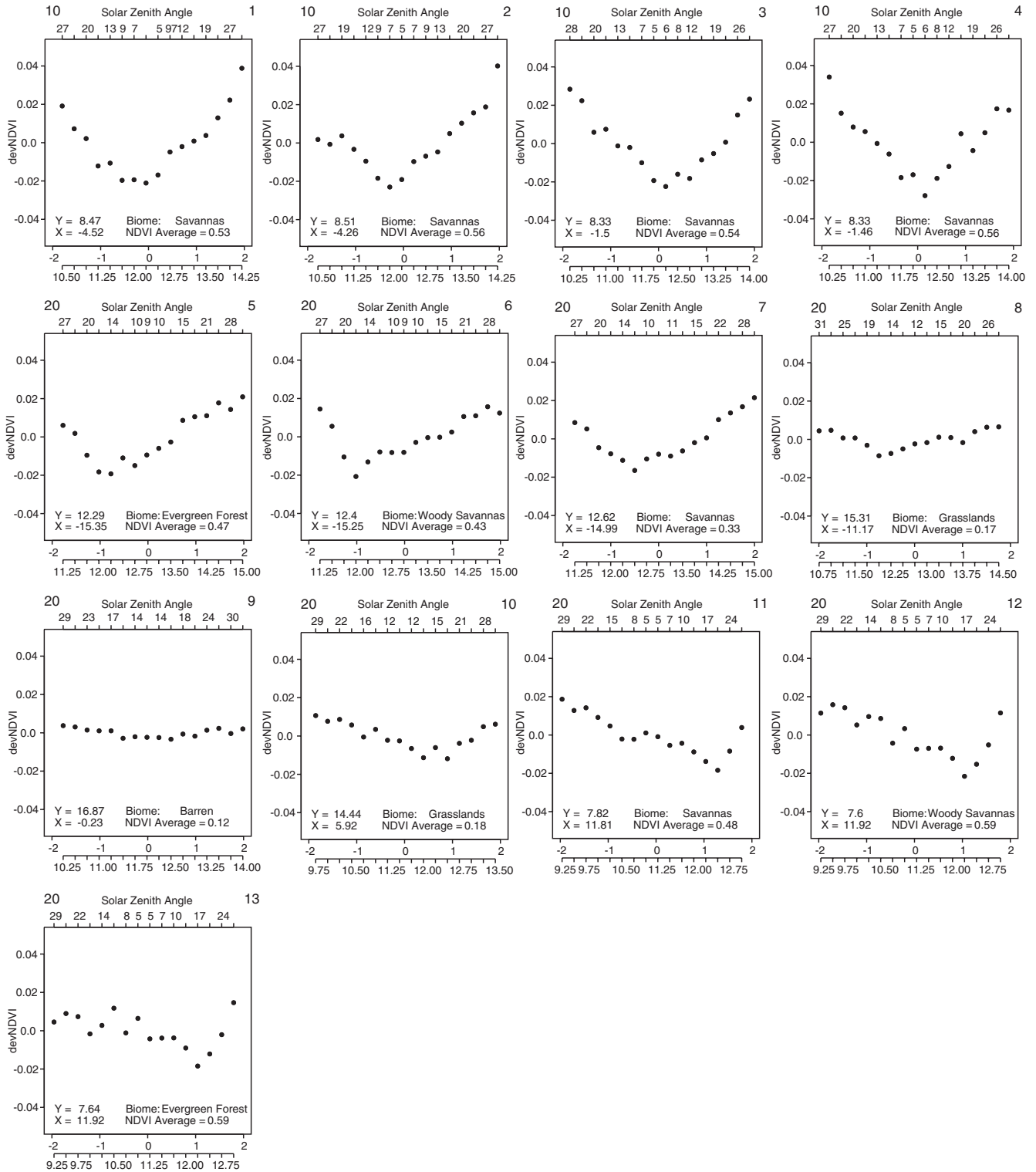
Fig. 8. Diurnal (29/3 2005) variation of MSG NDVI (plotted as deviations from the diurnal mean NDVI) for pixels with 10–20° sensor VZA's. Local time, GMT and solar zenith angles are indicated on x-axis. The numbers indicated to the upper right correspond to the numbers in Fig. 7b.

range is seen to decrease with decreasing vegetation intensity. The observed NDVI minimum has now shifted to be approximately one hour before local solar noon which corresponds very well with the location 12° west of the sensor (15 degrees equals one hour shift in local solar noon). Pixels 10–13 mirror the biome classes and vegetation intensities of the

pixels 5–8 plots. The geographic location is now app. 12° east of the sensor and the observed diurnal NDVI minimum has shifted towards one hour after local solar noon.

Selected plots are analyzed for diurnal variations in red and near-infrared reflectances (pixels 1, 3, 5, 9 and 11) to uncover the basis of the observed NDVI variations (Fig. 9). The red and
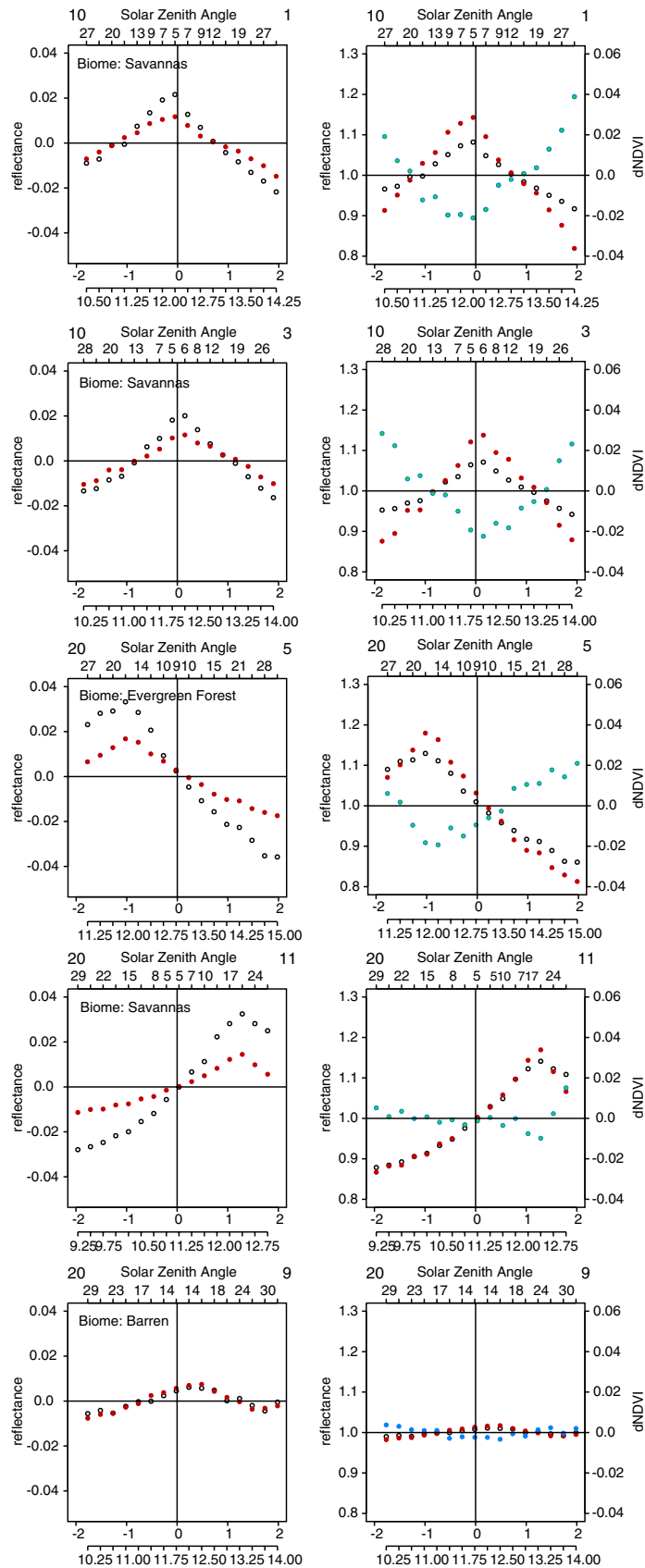
Fig. 9. Red (red) and near-infrared (open) diurnal (29/3 2005) reflectance plotted as differences from the average in absolute numbers (left panel) and as relative differences to the average (right panel). Diurnal NDVI (blue) is included in the right panel. The numbers indicated to the upper right correspond to the numbers in Fig. 7B.

near-infrared diurnal reflectances of the five selected pixels are given as differences from the simple average in absolute numbers in the left panel and as relative differences to the simple average in the right panel. Diurnal observed NDVI is included in the right panel. For all pixels the red and near-infrared reflectances exhibit a diurnal bell-shaped curve, characterized by maximum reflectance at backscatter conditions. In absolute values (left panel) the diurnal observed variations in near-infrared reflectances exceed the variations in red. However, the opposite is the case for relative diurnal reflectance variations because the level of red reflectance is considerably lower than near-infrared reflectance for vegetated surfaces due to chlorophyll absorption. This is in accordance with model studies reported in the literature, for instance Sandmeier and Itten (1998), Gao et al. (2002) have found lower anisotropy factors for near-infrared. The difference in anisotropic reflectance properties between red and near-infrared reflectances thus becomes apparent, causing the diurnal variations in observed NDVI. For

backscatter conditions the relative red reflectance becomes higher than the near-infrared reflectance causing the observed NDVI to decrease. Pixel 9 is characterized by bare soil and NDVI of 0.12 (biome type; barren or sparsely vegetated). The difference in diurnal variation between red and near-infrared reflectance is almost absent because this pixel is located almost perpendicular to the sun-sensor principal plane reducing the effect of forward/backward scatter induced variations.

4.3.2. Viewing angles from 30° to 50°

For MSG SEVIRI VZA's from 30°, 40° and 50° land pixels are only present east of the sensor. Pixels 14–18 (Fig. 10) along the 30° VZA line represent the five biome classes also covered by the 20° VZA line.

The same pattern as for 10° and 20° VZA's emerges with increasing diurnal observed NDVI amplitude as a function of vegetation density and now the diurnal observed NDVI minimum is at approximately 1 1/2 h after local solar noon;
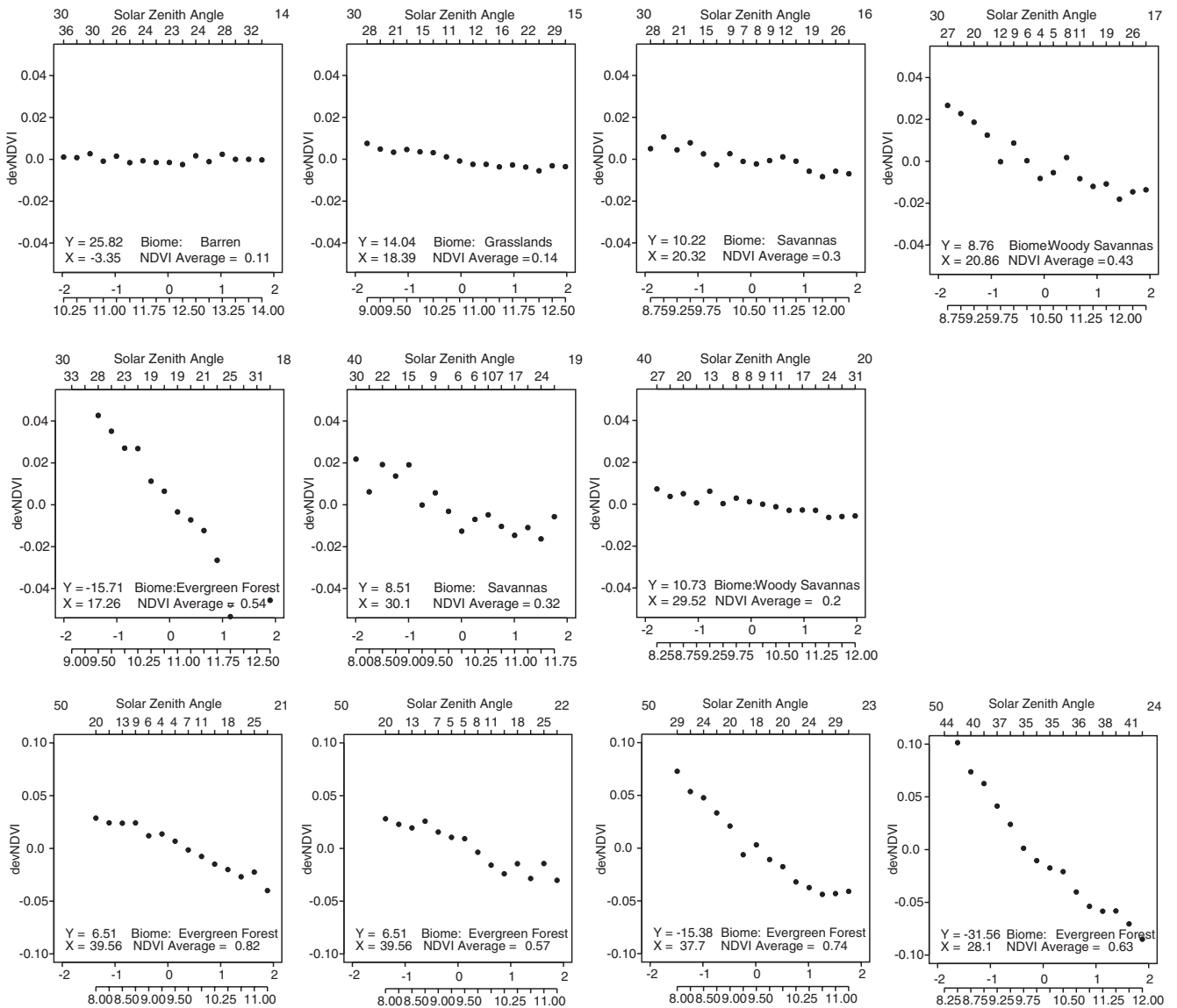
Fig. 10. As Fig. 8, but for pixels with 30–50° sensor VZA's.

corresponding to a pixel location of 20–25° east of the sensor. Plots of savannas and woody savannas (19 and 20) are given for VZA's of 40° (more dense vegetation plots were unavailable due to cloud cover) and diurnal observed NDVI minimum is now shifted towards the end of the 4 h window.

Pixels characterized by a 50° VZA (Fig. 10) generally show decreasing observed NDVI values throughout the 4 h window of analysis illustrating that the maximum backscatter condition appears after the cut-off at 2 pm local solar noon. All pixels (21–24) characterized by a 50° VZA are classified as broadleaf evergreen forest to illustrate the observed NDVI dynamic range dependency of the sun-sensor geometry (note that the value-axis dynamic range of the 50° VZA is larger than in earlier plots). The diurnal dynamic range of pixels 21 and 22 NDVI is 0.08 (average 0.82) and 0.06 (average 0.57). The geographic location is app. 42° east of the sensor causing a shift in local solar noon of almost 3 h compared to the sensor position. It means that maximum backscatter conditions are never reached within the 4 h window. Moving southward, the difference between local solar noon at the sensor and local solar noon at 50° VZA pixels decreases as a function of latitude on the southern hemisphere, meaning that maximum backscatter conditions again approach the proximity of the 4 h window. This is the case in pixel 24, where the combined effect of VZA's of 50°, a difference in local solar noon of only 2 h compared to the sensor and the fact that the trajectory of the sun on March 29 is north of the sensor provide conditions for an afternoon "hot spot" situation in southern Africa. A diurnal NDVI variation

of 0.2 in pixel 24 and 0.13 in pixel 23 supports these considerations. Fig. 11 is a map of daily range in observed NDVI normalized by its mean NDVI; only pixels, which are cloud free in the entire 4-h window, are included. The large relative range in daily observed NDVI-values found in the southern Africa region supports the hypothesis of "hot spot" conditions in southern Africa at that time of year, but at the same time, the southern and eastern parts of Africa with high view angles are located at the limit of the validity of the SMAC algorithm. Further analyses are clearly needed to substantiate these preliminary findings.

Anisotropy as a function of wavelength and cover type has been recognized for many years and the BRDF obviously both influences observed NDVI from Polar Orbiting Environmental Satellites (POES) and geostationary data. Since POES data encompasses variations in both sun and view zenith angles the nature of geometry induced reflectance variations is relatively complex and many applications disregard the angular effects on observed NDVI, which is the case for the widely used maximum value composite method. A MODIS Nadir BRDF-Adjusted Reflectance product is however produced on a 16-day basis correcting for variations in view and sun angles (MOD43B4) (Schaaf et al., 2002). A finer temporal resolution is not feasible because a minimum of 7 cloud free observations is needed to invert the model.

The results presented above present the new challenges of working with vegetation indices from the geostationary MSG SEVIRI where the importance of the diurnal sun-sensor geometry variation influence on observed surface reflectance
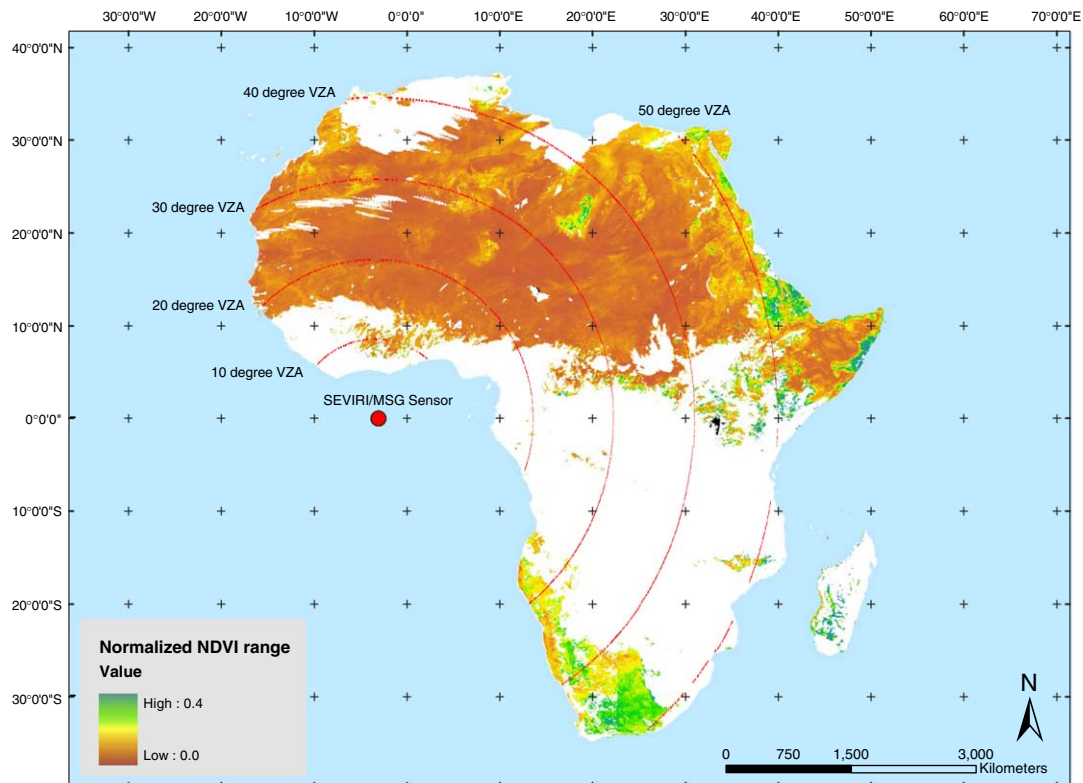
Fig. 11. Map of the normalized MSG NDVI diurnal range for pixels labelled as cloud free in the interval from 10 am to 2 pm local solar noon (29/3 2005). MSG Data c2005 EUMETSAT.

and NDVI is exposed. Data from the geostationary MSG SEVIRI sensor with a fixed position of the satellite sensor and only the sun moving composes a complementary information source to the POES data. The fundamental acquisition differences point towards different and complimentary use of these data sources. MSG NDVI data have an advantage when performing pixel by pixel time series analysis, like land change science etc. because of the fixed viewing geometry. A decrease in composite period length potentially leads to more accurate assessment of near real time vegetation development, which is decisive for e.g. early warning systems. On the contrary comparison of MSG NDVI in the spatial domain is more difficult (due to preservation of differences in view angles over the continent) if not corrected for. Future work will deal with a proper normalization of the MSG SEVIRI surface reflectance data before deriving NDVI. Due to the high temporal frequency of data it is likely that a correction modeling scheme will perform well thereby maintaining the benefit of the high temporal frequency. The variations in observed diurnal reflectances and NDVI from MSG SEVIRI can be regarded as noise, which should be removed performing solar zenith and azimuth normalization, but the observed diurnal variation can also be used to infer canopy structure and architecture information. The study of Diner et al. (2005) has demonstrated the potential of supplementing multispectral measurements with multi-angle measurements. Solving the general problem of anisotropy in NDVI monitoring requires a large amount of modeling; a research subject which can now be complemented by the MSG SEVIRI red and near-infrared reflectance data which can be a valuable complementary input to vegetation structure modeling from POLDER and MISR Fig. 12–14.

5. Conclusion

A new generation of Earth Observation data is now available from the SEVIRI instruments onboard the geostationary MSG satellite. MSG forms the first opportunity to study NDVI from a geostationary satellite by including both a red and near-infrared channel, thereby significantly improving the temporal resolution of NDVI data. This study points towards new challenges in NDVI monitoring exploiting the information content of the diurnal curves of NDVI for vegetation characterization. For the Dahra test site in Senegal, we have demonstrated that the temporal resolution of cloud free image acquisitions from MSG SEVIRI data is greatly improved (for the 2004 growing season 82 cloud free days from SEVIRI compared to 47 with MODIS, corresponding to a 79% increase) with the constraints of an observing window from 10 am to 2 pm. The implications for NDVI compositing are notable; a preliminary composite analysis including 10 am to 2 pm suggests that using 5 days composite periods of the African continent produces 95% cloud free pixels which typically would require 15–20 days of data from a polar orbiting satellite. More available NDVI data potentially will produce more accurate seasonal integrals of photosynthetic activity due to fewer problems related to cloud contamination. When comparing growing season MSG SEVIRI and MODIS NDVI for the test site, differences in BRDF were found to influence the time series of NDVI; MSG NDVI being higher than MODIS in July–August and lower in October–November.

For cloud free days, the diurnal variation in reflectance and thus vegetation indices can be detected based on MSG SEVIRI data, with solar zenith and azimuth angles as the only varying parameters, the viewing geometry of the scenes being constant. Diurnal MSG NDVI was compared to in situ measured MSG NDVI at the test site in Senegal and the same bowl-shaped diurnal curve was found for both data sources. The dynamic range of MSG observed NDVI was higher than in situ data indicating the effect of view angles. Time of diurnal minima for the two measurements is displaced by ~one hour. A "hot spot" situation for the MSG SEVIRI observation occurs at app. 10:45 local solar time, due to the position of the sensor 12° east of the pixel when the sun and sensor are in the principal plane. The local minimum for the nadir viewing in situ sensor occurs at ~12 local solar time, when the solar zenith is at its minimum.

The significance of reflectance differences between the red and near-infrared wavelengths due to differences in anisotropy becomes evident when studying diurnal observed NDVI of pixels characterized by different sensor view zenith angles and vegetation types. Analysis of the diurnal variation in observed NDVI for view angles varying from 10° to 50° clearly demonstrates the NDVI dependency of diurnal variations in solar zenith angles, view angle and green vegetation density. Further work needs to be done within the domain of BRDF modeling of the MSG reflectance data to produce daily values of MSG NDVI normalized for acquisition time. MSG SEVIRI data can by used to gain new insights in the dependence of observed NDVI on solar and viewing geometry, and this knowledge may be used in combination with data from the polar orbiting sensors like MISR, MODIS Terra and Aqua and the forthcoming EPS-AVHRR which all have varying viewing geometry to derive more robust, consistent and timely information about the vegetation cover of the Earth's surface.

References

Berthelot, B. (2003). Coefficients SMAC pour MSG. Technical Report, Noveltis Internal Report NOV-3066-NT-834.

Cihlar, J., Manak, D., & D'iorio, M. (1994). Evaluation of compositing algorithms for AVHRR data over land. *IEEE Transactions on Geoscience and Remote Sensing*, *32*, 427−437.

d'Entremont, R. P., Schaaf, C. B., Lucht, W., & Strahler, A. H. (1999). Retrieval of red spectral albedo and bidirectional reflectance using AVHRR HRPT and GOES satellite observations of the New England region. *Journal of Geophysical Research*, *104*(D6), 6229−6240.

Deering, D. W., Middleton, E. M., Irons, J. R., Blad, B. L., Walter-Shea, E. A., Hays, C. J., et al. (1992). Prairie grassland bidirectional reflectances measured by different instruments at the FIFE site. *Journal of Geophysical Research*, *97*, 18887−18903.

Deschamps, P. Y., Breon, F. M., Leroy, M., Podaire, A., Bricaud, A., Buriez, J. C., et al. (1994). The POLDER mission — Instrument characteristics and scientific objectives. *IEEE Transactions On Geoscience and Remote Sensing*, *32*(3), 598−615.

Diner, D. J., Beckert, J. C., Reilly, T. H., Bruegge, C. J., Conel, J. E., Kahn, R. A., et al. (1998). Multi-angle imaging spectroradiometer (MISR) — Instrument description and experiment overview. *IEEE Transactions on Geoscience and Remote Sensing*, *36*(4), 1072−1087.

Diner, D. J., Braswell, B. H., Davies, R., Gobron, N., Hu, J. N., Jin, Y. F., et al. (2005). The value of multiangle measurements for retrieving structurally and radiatively consistent properties of clouds, aerosols, and surfaces. *Remote Sensing of Environment*, *97*(4), 495−518.

Eklundh, L., & Olsson, L. (2003). Vegetation index trends for the African Sahel 1982−1999. *Geophysical Research Letters*, *30*(8), 1430−1433.

EUMETSAT (2004). EUMETCast. EUMETSAT's Broadcast System for Environmental Data. EUM TD 15, EUMETSAT.

EUMETSAT (2005). MSG level 1.5 image data format description. Technical Report.

Fensholt, R., & Sandholt, I. (2005). Validation of the MODIS and NOAA AVHRR vegetation indices with in situ measurements in a semi-arid environment. *International Journal of Remote Sensing*, *26*(12), 2561−2594.

Fensholt, R., Anyamba, A., Stisen, S., Sandholt, I., Pak, E., & Small, J. (submitted for publication). Comparisons of compositing period length for vegetation index data from Polar-orbiting and Geostationary satellites for the Cloud-prone region of West Africa. Submitted to Photogrammetric Engineering & Remote Sensing.

Gao, F. Y., Jin, X. L., Schaaf, C., & Strahler, A. H. (2002). Bidirectional NDVI and atmospherically resistant BRDF inversion for vegetation canopy. *IEEE Transactions of Geoscience and Remote Sensing*, *40*, 1269−1278.

Geiger, B., Franchisteguy, L., Lajas, D., & Roujean, J. -L. (2004). Operational near real-time derivation of land surface albedo and down-welling short-wave radiation from MSG observations. *Proc. second MSG RAO workshop, Salzburg, Austria. ESA SP 582*.

Gobron, N., Aussedat, O., Pinty, B., Taberner, M., & Verstraete, M. (2004). *Medium resolution imaging spectrometer (MERIS) — Level 2 land surface products algorithm theoretical basis document. (Revision 3)*.

Govaerts, Y., Wagner, S., Clerici, M., 2005. SEVIRI native format pre-processing toolbox. User's guide. Technical report EUM/OPS-MSG/TEN/03/0011, EUMETSAT, Am Kavalleriesand 31. Postbox 10 05 55. D-64205 Darmstadt.

Goward, S. N., & Hummrich, K. F. (1992). Vegetation canopy par absorptance and the normalized difference vegetation index; an assessment using sail model. *Remote Sensing of Environment*, *39*, 119−140.

Grant, I. F., Heyraud, C., & Breon, F. M. (2004). Continental scale hotspot observations of Australia at sub-degree angular resolution from POLDER. *International Journal of Remote Sensing*, *25*(18), 3625−3636.

Hansen, L. (2001). Chips development team. http://www.geogr.ku.dk/chips/index.htm

Hanson, C., & Mueller, J. (2004). Status of the SEVIRI level 1.5 data. *Proc. second MSG RAO workshop, Salzburg, Austria. ESA SP 582*.

Hapke, B., DiMucci, D., Nelson, R., & Smythe, W. (1996). The cause of the hot spot in vegetation canopies and soils: Shadow-hiding versus coherent backscatter. *Remote Sensing of Environment*, *58*, 63−68.

Hautecoeur, O., & Leroy, M. M. (1998). Surface bidirectional reflectance distribution function observed at global scale by POLDER/ADEOS. *Geophysical Research Letters*, *25*(22), 4197−4200.

Holben, B. N. (1986). Characteristics of maximum-value composite images for temporal AVHRR data. *International Journal of Remote Sensing*, *7*, 1435−1445.

Holben, B., & Fraser, R. (1984). Red and near-infrared sensor response to off-nadir viewing. *International Journal of Remote Sensing*, *5*(1), 145−160.

Huete, A., Didan, K., Miura, T., Rodriguez, E., Gao, X., & Ferreira, L. (2002). Overview of the radiometric and biophysical performance of the MODIS vegetation indices. *Remote Sensing of Environment*, *83*, 195−213.

Huete, A. R., Hua, G., Qi, J., Chehbouni, A., & van Leeuwen, W. J. D. (1992). Normalization of multidirectional red and NIR reflectance with the SAVI. *Remote Sensing of Environment*, *41*, 143−154.

Huete, A.R., Justice, C.O., Van Leeuwen, W.J.D., 1999. MODIS vegetation index (MOD 13). Version 3. Algorithm theoretical basis document. Technical report, http://modis.gsfc.nasa.gov/data/atbd/land atbd.html

James, M. E., & Kalluri, S. N. V. (1994). The pathfinder AVHRR land data set: An improved coarse resolution data set for terrestrial monitoring. *International Journal of Remote Sensing*, *15*, 3347−3363.

Kaufman, Y.J., Tanre, D. (1998). Algorithm for remote sensing of tropospheric aerosol from MODIS, algorithm theoretical basis document. Technical report ATBD-MYD-02, NASA Goddard Space Flight Center.

Lacaze, R., Jing, M. C., Roujean, J. L., & Leblanc, S. G. (2002). Retrieval of vegetation clumping index using hot spot signatures measured by POLDER instrument. *Remote Sensing of Environment*, *79*(1), 84−95.

Leroy, M., Deuze, J. L., Breon, F. M., Hautecoeur, O., Herman, M., Buriez, J. C., et al. (1997). Retrieval of atmospheric properties and surface bidirectional reflectances over land from POLDER/ADEOS. *Journal of Geophysical Research—Atmospheres*, *102*(D14), 17023−17037.

Li, X., & Strahler, A. H. (1986). Geometric-optical bidirectional reflectance modeling of a conifer forest canopy. *IEEE Transactions on Geoscience and Remote Sensing*, *24*(6), 906−919.

Loveland, T., & Belward, A. (1997). The IGBP-DIS global 1 km land cover data set, discover first results. *International Journal of Remote Sensing*, *18*(5), 3289−3295.

Menzel, W.P., Gumley, L.E. (1998). MODIS atmospheric profiles retrieval algorithm theoretical basis document. Technical report ATBD-MYD-07, NASA Goddard Space Flight Center.

Myneni, R., Asrar, G., & Hall, F. G. (1992). A three dimensional radiative transfer method for optical remote sensing of vegetated land surfaces. *Remote Sensing of Environment*, *41*, 105−121.

Myneni, R. B., Hall, F. G., Sellers, P. J., & Marshak, A. L. (1995). The interpretation of spectral vegetation indexes. *IEEE Transactions on Geoscience and Remote Sensing*, *33*, 481−486.

Nemani, R. R., Keeling, C. D., Hashimote, H., Jolly, W. M., Piper, S. C., Tucker, C. J., et al. (2003). Climate-driven increases in global terrestrial net primary production from 1982 to 1999. *Science*, *300*, 1560−1563.

Pinty, B., Widlowski, J. -L., Gobron, N., Verstraete, M. M., & Diner, D. J. (2002). Uniqueness of multiangular measurements part 1: An indicator of subpixel surface heterogeneity from MISR. *IEEE Transactions on Geoscience and Remote Sensing*, *40*, 1560−1573.

Pokrovsky, I., Pokrovsky, O., & Roujean, J. -L. (2003). Development of an operational procedure to estimate surface albedo from the SEVIRI/MSG observing system by using POLDER BRDF measurements. I. Data quality control and accumulation of information corresponding to the IGBP land cover classes. *Remote Sensing of Environment*, *87*, 198−214.

Rahman, H., & Dedieu, G. (1994). SMAC: A simplified method for the atmospheric correction of satellite measurements in the solar spectrum. *International Journal of Remote Sensing*, *15*(1), 123−143.

Roberts, G. (2001). A review of the application of BRDF models to infer land cover parameters at regional and global scales. *Progress in Physical Geography*, *25*, 483−511.

Sandmeier, S., & Itten, K. (1998). Physical mechanisms in hyperspectral BRDF data of grass and watercress. *Remote Sensing of Environment*, *66*, 222−233.

Schaaf, C. B., Gao, F., Strahler, A. H., Lucht, W., Li, X., Tsang, T., et al. (2002). First operational BRDF, albedo and nadir reflectance products from MODIS. *Remote Sensing of Environment*, *83*, 135−148.

Schmetz, J., Pili, P., Tjemkes, S., Just, D., Kerkman, J., Rota, S., et al. (2002). An introduction to meteosat second generation (MSG). *Bulletin of American Meteorological Society*, 977−992.

SPOT vegetation user's guide http://vegetation.cnes.fr/system/content.html#userguide (Accessed May 2004).

Taylor, D. (2005). MSG data manager pro homepage. http://www.satsignal.net/

Teianu, B., Hanson, C. G., Just, D., Lancashire, D., Mˆuller, J., & Raval, P. (2004). Meteosat-8 (MSG-1) SEVIRI performance during the commissioning and initial routine operations phases. *The 2004 EUMETSAT meteorological satellite conference*Prague, Czech Republic, 31.05.-04.06.2004.

Tucker, C. J. (1979). Red and photographic infrared linear combinations for monitoring vegetation. *Remote Sensing of Environment*, *8*, 127−150.

Tucker, C. J., Pinzon, J. E., Brown, M. E., Slayback, D., Pak, E. W., Mahoney, R., et. al. (in press). An extended AVHRR 8-km NDVI data set compatible with MODIS and SPOT vegetation NDVI data.

van Leeuwen, W. J. D., & Roujean, J. -L. (2002). Land surface albedo from the synergistic use of polar (EPS) and geo-stationary (MSG) observing systems. An assessment of physical uncertainties. *Remote Sensing of Environment*, *81*, 273−289.

Widlowski, J. -L., Pinty, B., Gobron, N., Verstraete, M., Diner, D., & Davis, A. (2004). Canopy structure parameters derived from multi-angular remote sensing data for terrestrial carbon studies. *Climatic Change*, *67*(2−3), 403−415.